Supporting Information

Humidity-Responsive Phase Transition and On-Demand UV-Curing in a Hygroscopic Polysiloxane-Surfactant Nanohybrid Film

Mitsuo Hara,[1] Taiki Orito,[1] Shusaku Nagano,[2] and Takahiro Seki*[1]

[1]Department of Molecular and Macromolecular Chemistry, Graduate School of Engineering, Nagoya University, Furo-cho, Chikusa-ku, Nagoya, Aichi, Japan 464-8603

[2]Nagoya University Venture Business Laboratory, Furo-cho, Chikusa-ku, Nagoya, Aichi, Japan 464-8603

Materials

3-Aminopropyldimethoxymethylsilane (APDMOS), dimethoxymethylvinyl-silane (VDMOS), 1-[4-(2-hydroxyethoxy)-phenyl]-2-hydroxy-2-methyl-1-propane (Irgacure® 2959, I2959), DL-dithiothreitol (DTT) were purchased from Tokyo Chemical Industry Co., Ltd. Cetyltrimethylammmonium bromide (CTAB), tetraethoxysilane (TEOS), ethanol (EtOH), methanol, concentrated hydrochloric acid (HCl) were purchased from Kanto Chemical Co., Inc. All reagents used were commercial purities. Pure water (PW) was obtained by a Direct-Q® 3UV purification system (Millipore Corp., ρ>18 MΩ·cm at 25 °C).

Silica precursor solution was prepared by sol-gel reaction of TEOS as below. The solution composed of TEOS, PW, EtOH, and HCl was stirred at 70 °C for 2h. The molar ratio of the components in this solution was TEOS (1): PW (5): EtOH (5): HCl (0.05).

Synthesis of water-absorbing polysiloxane PSAV

A siloxane copolymer PSAV, which contains an amine-hydrochloride group and a vinyl group, was synthesized by hydrolysis and polycondensation of APDMOS and VDMOS according to the report by Kaneko et al.[1] 0.41 g of APDMOS (2.5 mmol), 0.15 g of VDMOS (1.1 mmol), and 25.7 g of 0.5 mol·dm^{-3} HCl were placed into a brown glass bottle. This mixture was stirred at r.t. until all of the solvent evaporated (stirring rate: 600 rpm). Residual viscous solid was re-dissolved in a small portion of

PW and freeze-dried for overnight, then PSAV was obtained in 44.7% yield (0.21 g). ^{1}H NMR measurements were performed by a FT-NMR spectrometer JNM-A400 (JEOL Ltd.). ^{1}H NMR spectrum was shown in Figure S1 (400 MHz, deuterium oxide): δ (ppm) 0.22−0.28 (s+s, 3.6H, C<u>H</u>$_3$-Si-CH$_2$CH$_2$CH$_2$NH$_3^+$Cl$^-$ and C<u>H</u>$_3$-Si-CH=CH$_2$), 0.66 (s, 2H, CH$_3$-Si-C<u>H</u>$_2$CH$_2$CH$_2$NH$_3^+$Cl$^-$), 1.73 (s, 2H, CH$_3$-Si-CH$_2$C<u>H</u>$_2$CH$_2$NH$_3^+$Cl$^-$), 3.00 (s, 2H, CH$_3$-Si-CH$_2$CH$_2$C<u>H</u>$_2$NH$_3^+$Cl$^-$), 5.95 (s, 0.2H, CH$_3$-Si-C<u>H</u>=CH$_2$), 6.11 (s, 0.4H, CH$_3$-Si-CH=C<u>H</u>$_2$).

The molar ratio of each unit in the copolymer was APDMOS:VDMOS = 5:1, which was calculated from the peak-integration ratio of δ = 3.00 and 6.11 ppm in ^{1}H NMR spectrum.

Additionally, the copolymer PSAV was characterized by a size exclusion chromatography (SEC). The SEC measurement was taken by HPLC pump GL-7410 (GL Sciences Inc.), RI detector GL-7454 (GL Sciences Inc.), GPC column Shodex® GPC K-803 and K-804 (Showa Denko K.K., polymethyl methacrylate standards in *N*,*N*-dimethylformamide (DMF)). As a pretreatment for the SEC measurement, PSAV was mixed into DMF, then triethylamine and 2-bromoethanol were added into the PSAV-DMF solution to dissolve PSAV. Bimodal signal was obtained corresponding to M_n = 4.8×10^3 and 1.4×10^3) with M_w/M_n = 1.4. Minor signal (M_n = 1.4×10^3) is assignable to an oligomer or a ring polymer formation.

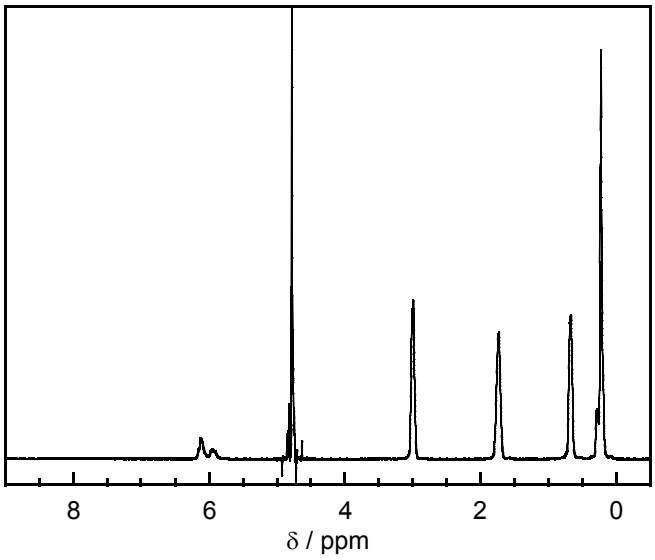

Figure S1. ^{1}H NMR spectrum of PSAV.

Measurements

Film samples were prepared by a spin-coating method using a K-359S1 (Kyowariken Co., Ltd.). Solution was dropped onto substrates, the substrates were then spun at 2000 rpm for 30 s. Film thicknesses and surface roughnesses of the films and were characterized by an optical microscope using a focus variation with white light interferometry BW-S507-N (Nikon Corp.) at room temperature and ambient humidity (generally 30−60% RH).

Quartz crystal microbalance (QCM) measurements were carried out using a QCM monitor THQ-100P-SW equipped with a QCM electrode SEN-5P-10 (Tamadevice Co., Ltd., a resonance frequency of 5 MHz). Film samples were prepared onto the QCM electrode substrates by the spin-coating method and the sample was placed in an incubator ICI-1 (As One Corp.). All measurements were performed at 30 °C. A relative humidity was controlled by a steam-generation unit BELLFlow-1 (MicrotracBEL Corp.) and monitored with a temperature and humidity recorder RTR-503 (T&D Corp.).

Thermogravimetric (TG) analyses were performed by an EXSTAR 6000 equipped with TG/DTA 6200 (Seiko Instruments Inc.). About 10-mg powder samples were put into aluminum pans, the pans then were inserted into the instrument's N_2 atmosphere. Before the TG data were collected, an aging at 100 °C for 30 min to remove absorbed water. Successively, the pans were heated at a rate of 5 °C·min^{-1} until 230 °C and held at the temperature for 2 h.

Grazing-incidence X-ray diffraction (GI-XRD) measurements were taken by an X-ray diffractometer FR-E equipped with a two-dimensional detector R-axis IV (Rigaku Corp.) involving an imaging plate (Fujifilm Corp.). Beam of 0.3-mm collimated Cu Kα radiation (λ = 0.154 nm) was used as an X-ray, and the camera length was set at 300 mm. Film samples were placed onto a pulse motor stage and covered with a handmade chamber to control a relative humidity around the samples. An incident angle of the beam to the substrate surface was adjusted at ca. 0.18−0.22° by using a Z pulse motor stage ALV-300-HM and an oblique pulse motor stage ATS-C310-EM (Chuo Precision Industrial Co., Ltd.). Humidity in the chamber was controlled by BELLFlow-1 and monitored by RTR-503. X-ray radiation was started 10-min after the humidity in the chamber reached into the setting value and X-ray exposed time was generally set at 10 min. For irradiation of a UV light, a mercury lamp UVF-204S (San-ei Electric Co., Ltd.) was used. A wavelength below 310 nm was cut by glass slide and a light intensity was set to 20 mW·cm^{-2} converted at λ = 365 nm, which detected with an optical power meter TQ8210 attached with an optical sensor Q82017

(ADC Corp.).

Film thickness and morphology

Figure S2a displays an exterior view of the CTAB-PSAV hybrid film. The film was transparency as well as printed letters can be fully viewed through the film. The CTAB-PSAV hybrid film was observed by microscopic images using a focus variation with white light interferometry (BW-S507-N, Nikon Corp.) (Figure S2b). The vertical trench at the center was formed as a result of a scratch of the film. The height differences of the film in the average height profiles corresponds to film thickness; ca. 330 nm. The film had flat surface for their own thickness, but was observed a circular domain with the diameter of ca. 100 μm. This circular domain seems to be derived from a macro-phase separation of CTAB and PSAV because CTAB exhibits crystal phase at ambient humidity.

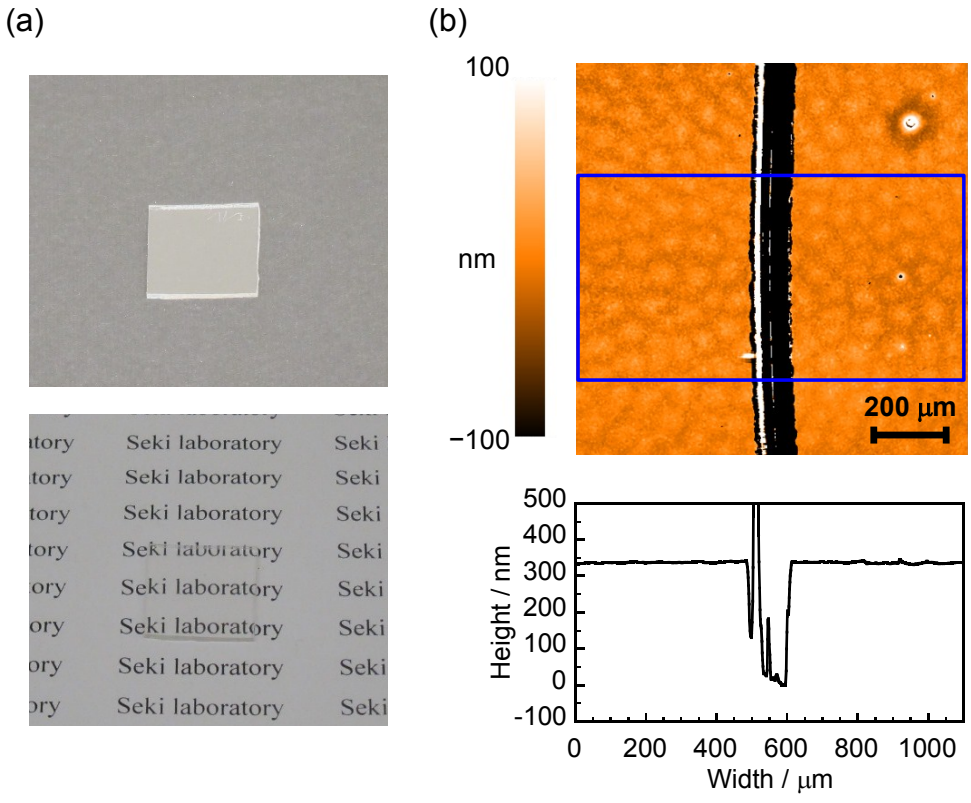

Figure S2. (a) Photos of the CTAB-PSAV hybrid films on black paper (top) and printed white paper (bottom). The films were prepared onto a 15 mm^2-size glass substrate. (b) Optical microscope image taken a 1.1 mm × 1.1 mm area of the CTAB-PSAV hybrid film and an average height profile in the area marked with blue square in the image.

Blank test of QCM measurement

QCM measurement of a bare QCM electrode was recorded in Figure S3. The weight changes were not observed during the measurement, indicating that the bare electrode did not absorb water at all.

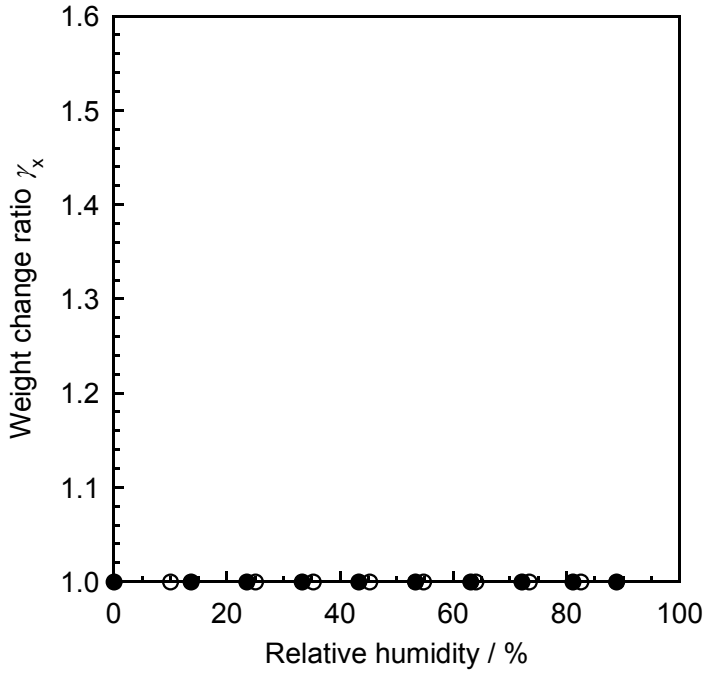

Figure S3. Weight changes of the bare QCM electrode on humidification process (filled) and dehumidification process (open).

Confirmation of thiol-ene reaction

A reactivity of thiol-ene click chemistry in this work was confirmed by ^{1}H NMR measurements (Figure S4). Although a deuterium oxide solution of a pure PSAV was irradiated UV irradiation with an intensity of 5 mW·cm^{-2} converted at λ = 365 nm for 100 s, the peaks derived from the vinyl group around 6 ppm were not disappeared. A mixture of PSAV and DTT also had the peaks of the vinyl group after UV irradiation. In a mixture of PSAV, DTT, and I2959, however, the peaks were disappeared after UV irradiation, indicating that the photo-induced thiol-ene reaction between PSAV and DTT proceeded successfully.

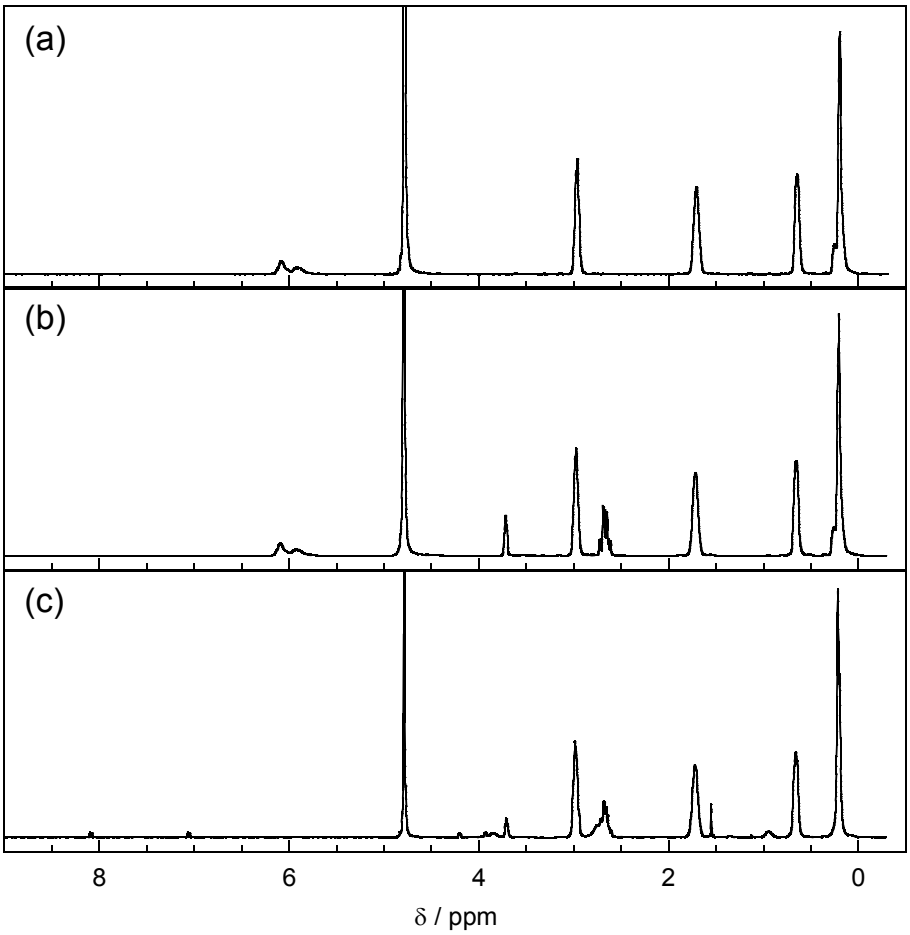

Figure S4. ^{1}H NMR spectra after UV irradiation. (a) A pure PSAV, (b) a mixture of PSAV and DTT (15:3 by weight), and (c) a mixture of PSAV, DTT, and I2959 (15:3:1 by weight).

Mixture ratio of organic-inorganic components in the hybrid film

An organic (CTAB) contents in the CTAB-PSAV hybrid film at various relative humidity were calculated based on one at 0% RH in the following way. First, we checked a thermal stability of CTAB and PSAV by TG analyses. The TG data under heating at 230 °C for 2h suggested that the calcination caused thermal decomposition almost all of CTAB molecules (≈99%) and ca. 2% of PSAV (Figure S5). The result indicates that the CTAB content in the CTAB-PSAV hybrid film can be calculated from the TG and QCM data.

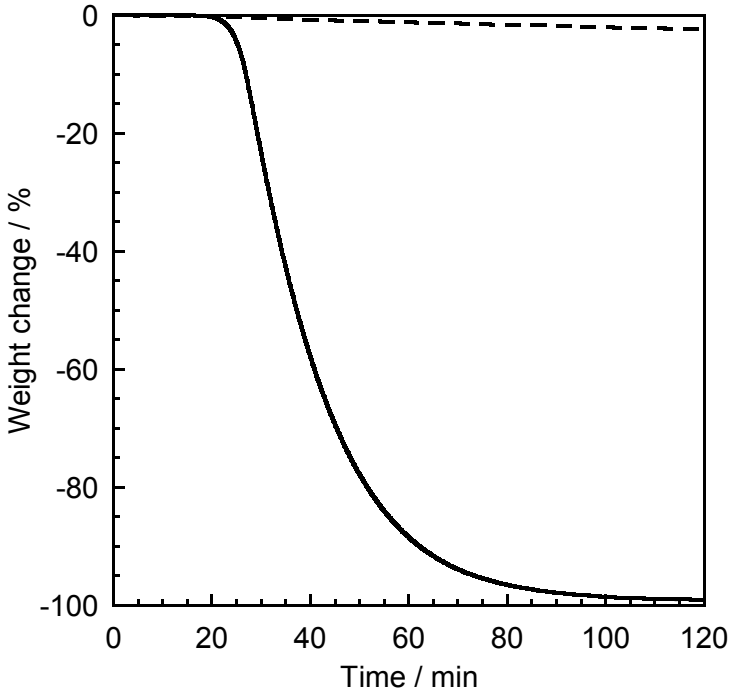

Figure S5. Thermal decomposition behaviors of CTAB (solid line) and PSAV (dashed line) at 230 °C.

Here, the CTAB concentration in the hybrid film at 0% RH is defined as $m_{CTAB,0}$. By means of the results of the QCM measurement, the $m_{CTAB,0}$ is estimated by the following equation,

$$m_{CTAB,0}\ (\text{wt \%}) = 100\times(m_{total,0} - 1.02\times m_{cal,0})/m_{total,0} \qquad \text{(eq. 1)}$$

where $m_{total,0}$ and $m_{cal,0}$ represent spincast film weights at 0% RH before and after calcination at 230 °C for 2h, respectively. The $m_{total,0}$ is obtained by subtracting a pure electrode substrate weight (before spin-coating of the CTAB-PSAV hybrid) from the CTAB-PSAV spincast film weight at 0% RH. The $m_{cal,0}$ is also obtained by subtracting the pure electrode substrate weight from the calcinated film weight at 0% RH. As a result, we calculated the $m_{CTAB,0}$ as 74 wt %, meaning that a content ratio in the hybrid film at 0% RH was determined as PSAV:CTAB = 1:3 by weight.

When the CTAB concentrations in the hybrid film at other relative humidity are defined as $m_{CTAB,x}$ with the subscript x being the relative humidity, the following equation is led,

$$m_{CTAB,x}\ (\text{wt \%}) = (m_{CTAB,0})/\gamma_x \qquad \text{(eq. 2)}$$

where γ_x is the weight change ratio, which is already defined and calculated in the main manuscript (Figure 2a, circles). We plotted the calculated $m_{CTAB,x}$ as triangles in Figure 2a. Moreover, the $m_{CTAB,x}$ at 0, 50, and 90% RH are indicated in Figure 2b of the main text.

GI-XRD detail profiles

Figure S6 depicts the humidity-controlled GI-XRD images of the CTAB-PSAV hybrid films on glass substrates. The hybrid film at 50% RH on humidification process showed the lamellae diffractions, which indicated as (001), (002), (003), and (004), in the out-of-plane direction to the substrate surface at $2\theta_y = 0°$. Many peaks also were observed in the wide-angle region, suggesting formation of crystalline lamellae structure. After moving the humidity up to 90% RH, the hybrid film changed its diffractions. No peak was observed in the wide-angle region. Moreover, the film gave many diffraction peaks with the *d*-spacing of ca. 4.4 nm on the same azimuth angle and its second-ordered peak (d = 2.5 nm). As the ratio of d values was $1:1/\sqrt{3}$, their peaks seem to be attributed to the hexagonal structure. Figure S7b displays an azimuth angle

(ϕ) profile at $2\theta = 2°$ ($d = 4.4$ nm) shown in Figure S7a. The peaks at intervals of $\phi =$ ca. 30° indicate existence of two alignments of hexagonal phases, that is there are two hexagonal phases which the (100) plane aligns to parallel and perpendicular to the substrate surface.[2] Note that two peaks ($\phi = 77°$ and $-78°$) nearby in-plane line should be exactly observed at $\phi = 90°$ and $-90°$, respectively. The differences are derived from lifting the substrate edge due to tilt of the film to the X-ray beam. After dehumidification down to 50% RH, the hybrid film had the crystalline lamellae structure which was almost the same one at first 50% RH.

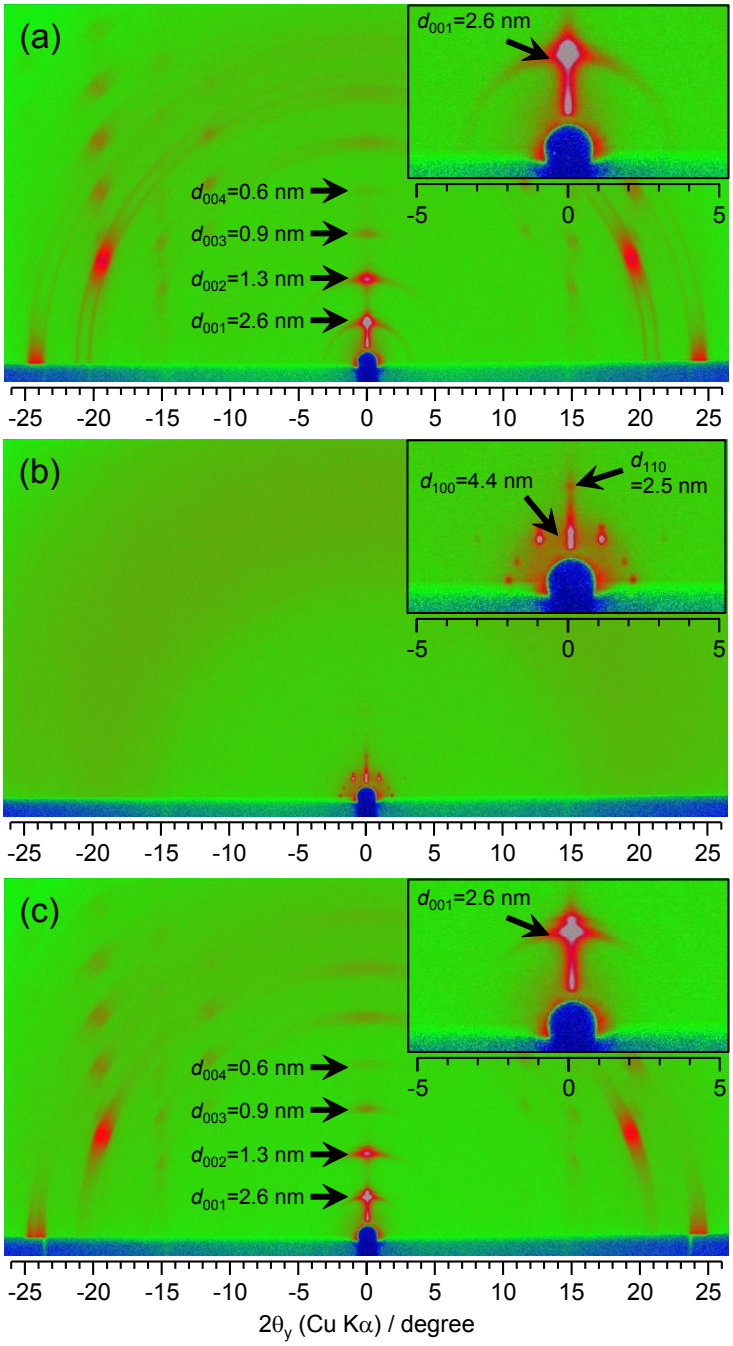

Figure S6. Humidity-controlled GI-XRD images of the CTAB-PSAV hybrid films at a relative humidity of 50% (a), 90% (b) on humidification process and 50% (c) on dehumidification process. The Insets display a magnified view in the small-angle region.

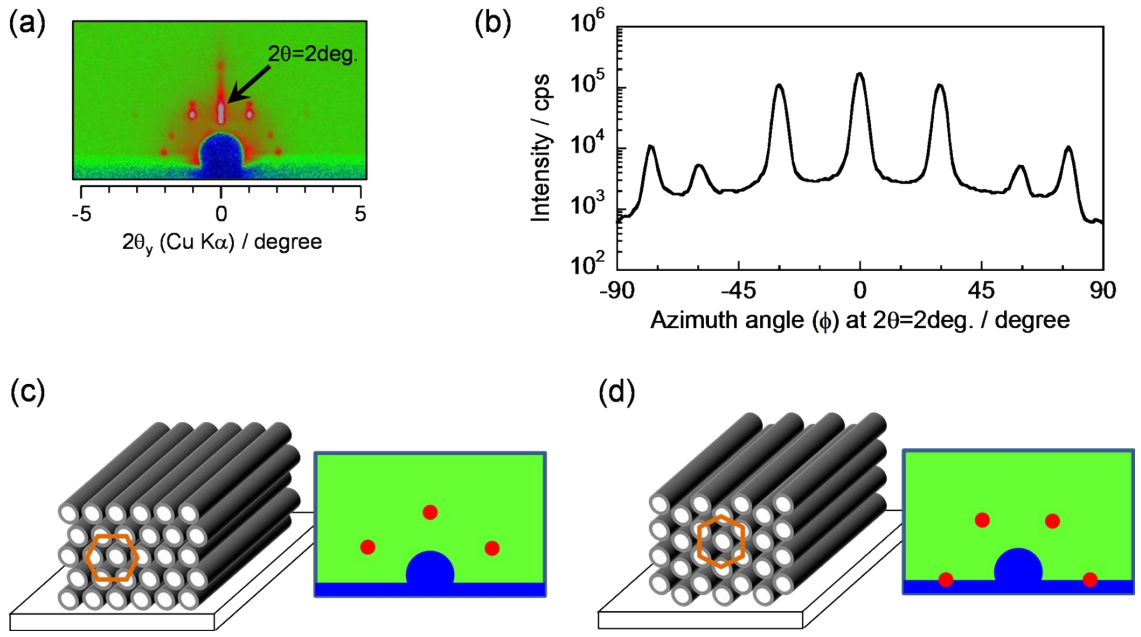

Figure S7. (a) GI-XRD image of the CTAB-PSAV hybrid film at 90% RH (same datum shown in Figure S6b). (b) Azimuth angle (ϕ) profile at 2θ=2deg. of a. The directions of 0, 3, and 9 o'clock in a correspond to ϕ=0, 90, and −90 degree in b, respectively. (c, d) Plausible hexagonal phases and its corresponding diffraction images. The (100) plane aligns parallel (c) and perpendicular (d) to the substrate surface.

As shown in Figure S8a (50% RH) and S8b (90% RH), the hybrid films containing DTT and I2959 exhibited the similar diffractions of corresponding them without DTT and I2959 at corresponding humidity. The (110) peak was not observed in the out-of-plane direction because the hexagonal structure preferred parallel orientation drawn in Figure S7c. On dehumidification down to 50% RH after UV irradiation at 90% RH, however the hybrid film had not the crystalline lamella but hexagonal structure. Appearance of hexagonal structure at 50% RH indicates that the CTAB aggregates were fixed due to the thiol-ene reaction.

References

1. Y. Kaneko, N. Iyi, K. Kurashima, T. Matsumoto, T. Fujita, K. Kitamura, *Chem. Mater.*, 2004, **16**, 3417-3423.

2. M. Knaapila, R. Stepanyan, B. P. Lyons, M. Torkkeli, A. P. Monkman, *Adv. Funct. Mater.* 2006, **16**, 599.

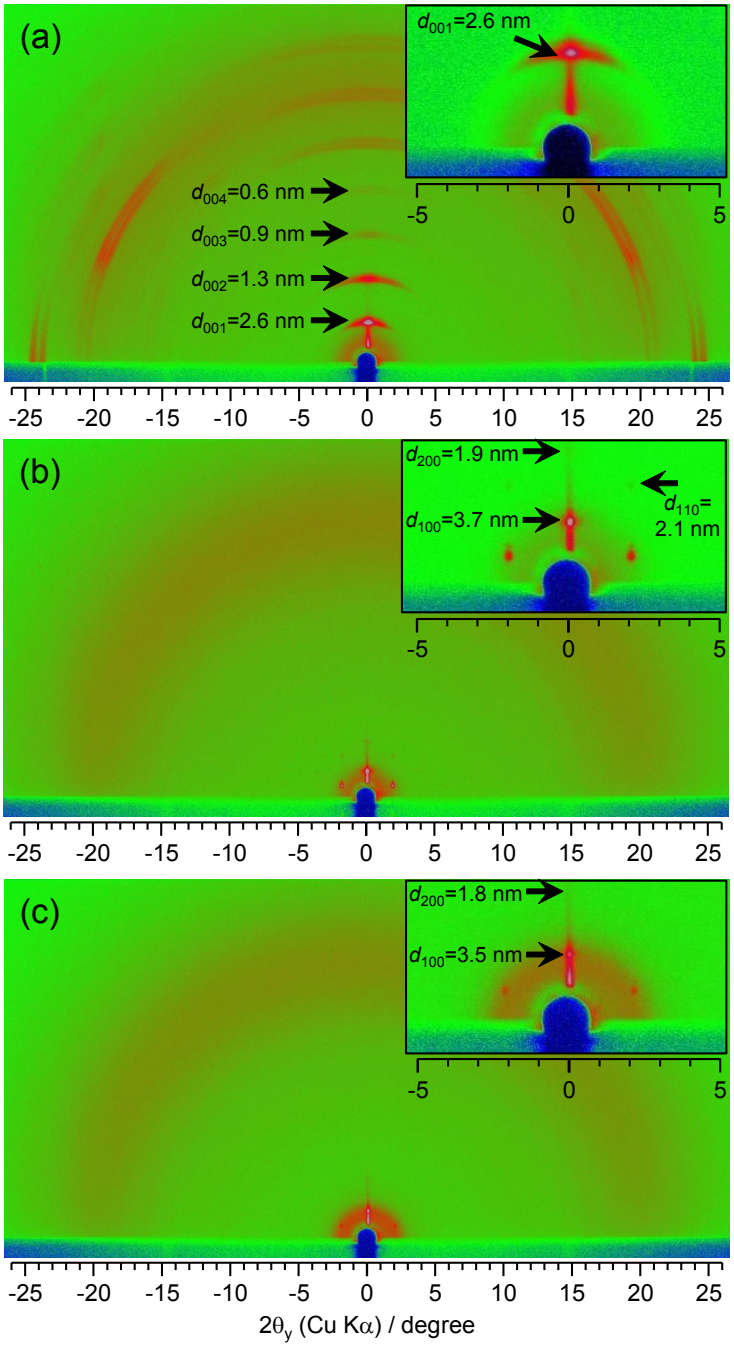

Figure S8. Humidity-controlled GI-XRD images of the CTAB-PSAV hybrid films containing a cross-linker DTT and an initiator I2959 at a relative humidity of 50% (a), 90% (b) on humidification process and 50% (c) on dehumidification process after UV irradiation at 90% RH. The insets display a magnified view in the small-angle region.